

# Calibrated birth-death phylogenetic time-tree priors for Bayesian inference

Joseph Heled<sup>\*1</sup> and A. J. Drummond<sup>†1,2</sup>

<sup>1</sup>Department of Computer Science, The University of Auckland, Auckland, New Zealand

<sup>2</sup>Allan Wilson Centre for Molecular Ecology and Evolution, New Zealand

November 21, 2013

## Abstract

Here we introduce a general class of multiple calibration birth-death tree priors for use in Bayesian phylogenetic inference. All tree priors in this class separate ancestral node heights into a set of “calibrated nodes” and “uncalibrated nodes” such that the marginal distribution of the calibrated nodes is user-specified whereas the density ratio of the birth-death prior is retained for trees with equal values for the calibrated nodes.

We describe two formulations, one in which the calibration information informs the prior on ranked tree topologies, through the (conditional) prior, and the other which factorizes the prior on divergence times and ranked topologies, thus allowing uniform, or any arbitrary prior distribution on ranked topologies. While the first of these formulations has some attractive properties the algorithm we present for computing its prior density is computationally intensive. On the other hand, the second formulation is always computationally efficient. We demonstrate the utility of the new class of multiple-calibration tree priors using both small simulations and a real-world analysis and compare the results to existing schemes.

The two new calibrated tree priors described in this paper offer greater flexibility and control of prior specification in calibrated time-tree inference and divergence time dating, and will remove the need for indirect approaches to the assessment of the combined effect of calibration densities and tree process priors in Bayesian phylogenetic inference.

**Keywords:** Bayesian Inference, Multiple Calibrations, BEAST, Yule Prior, Birth-death tree prior.

---

<sup>\*</sup>jheled@gmail.com

<sup>†</sup>alexexi@cs.auckland.ac.nz

# 1 Introduction

Divergence time dating and phylogenetic inference are related concerns. Recent advances in Bayesian phylogenetic inference [Rannala and Yang, 1996, Yang and Rannala, 1997, Huelsenbeck and Ronquist, 2001, Drummond and Rambaut, 2007] have culminated in the field of relaxed phylogenetic inference, in which both divergence times and phylogenetic relationships are simultaneously estimated [Drummond et al., 2006]. This estimation is aided by relaxed molecular clocks [Thorne et al., 1998, Kishino et al., 2001, Thorne and Kishino, 2002, Drummond et al., 2006, Rannala and Yang, 2007] which reconcile non-clock-like evolution with an underlying time-tree in which common ancestors are placed on an axis of time. In order to produce results on an absolute time scale it is necessary to either provide information on the rate of molecular evolution or alternatively calibrate a subset of internal nodes with a calibration density [Thorne et al., 1998, Yang and Rannala, 2006, Drummond et al., 2006]. Either way, In a Bayesian setting, a *tree process prior* must also be placed on all the uncalibrated divergence times. Arguably the simplest tree process priors are the one-parameter Yule model [Yule, 1924] and the two-parameter birth-death model [Nee et al., 1994b, Gernhard, 2008]. The latter has been suggested as an appropriate null model for species diversification Nee et al. [1994a] and has been extended to include additional parameters to model various types of incomplete sampling [Yang and Rannala, 1997, Stadler, 2009a, Höhna et al., 2011].

In a Bayesian setting, combining a calibration density (on one or more divergences) with a tree process prior into a single calibrated tree prior for divergence time estimation possesses a number of subtleties worthy of note, which we cover under the following headings.

## 1.1 Fossil bounds on a single divergence

Consider the simplest type of calibration to admit uncertainty: the placement of an upper and a lower limit on the age of a single monophyletic calibrated divergence ( $h_C$ ) in the tree:

$$\rho_h(h_C) = \begin{cases} 1/(u-l) & l \leq h_C \leq u \\ 0 & \text{otherwise} \end{cases} \quad (1)$$

This simple approach to calibration already has two quite distinct interpretations in a Bayesian setting when considered within the context of an overall tree prior on all divergence times. One interpretation is that the resulting marginal prior distribution on the calibrated divergence should obey the tree process prior (e.g. Yule or birth-death) but be constrained to be within the upper and lower bounds, so that the full calibrated tree prior,  $\rho_G(\cdot)$ , is:

$$\rho_G(h, \psi | \Lambda) \propto f_G(h, \psi | \Lambda) \rho_h(h_C), \quad (2)$$

where  $h$  represents the set of all divergence times,  $\psi$  is the ranked tree topology and  $\Lambda$  represents the parameter(s) of the tree process prior. The interpretation above was the only one available in the BEAST software until recently [Heled and Drummond, 2012]. An alternative “conditional-on-calibrated-node-ages” interpretation is that the marginal prior on the calibrated divergence should be uniform between the upper and lower limits and the prior on the remaining divergence times should follow the tree process prior,  $f_G(h, \psi | \Lambda)$ , conditioned on the height of the calibrated node [Yang and Rannala, 2006]:

$$\rho_G(h, \psi | \Lambda) = f_G(h \setminus h_C, \psi | \Lambda) \rho_h(h_C), \quad (3)$$

There is a difference between these two prior formulations regardless of whether the tree topology is known or estimated. In previous work Heled and Drummond (2012) described how to efficiently compute the latter formulation in the face of uncertainty in tree topology for arbitrary single-divergence calibration densities under the Yule tree prior.

## 1.2 *Nested calibrations*

It has been routine in almost all treatments of phylogenetic calibration so far to specify independent univariate priors for each calibrated divergence time. However calibrated divergence times that are nested in the tree are necessarily interdependent, such that the more recent calibrated divergence of a nested pair must be younger than the older calibrated divergence. If the specified calibration densities overlap then the resulting marginals of the joint prior will necessarily differ from the specified calibration densities. Nothing we present in this paper can correct for this. The correct solution to this problem is to specify a joint prior on the calibrated nodes that obeys the necessary condition that nested nodes are order statistics and therefore not free to vary independently.

## 1.3 *The influence of calibrations on the tree topology prior*

Heled and Drummond [2012] demonstrated that a natural interpretation of the “conditional-on-calibrated-age” construction of a calibrated tree prior produces a distribution that is non-uniform on ranked topologies. However we show in this paper that the tree prior can be decomposed into a prior on the node ages (both calibrated and uncalibrated) and a prior on the set of possible ranked histories. We show that this provides a means to compute a tree prior rapidly if a uniform prior on ranked trees is chosen. We compare this approach to a computational intensive alternative that weighs each ranked tree topology by its probability conditional on the divergence times of the calibrated nodes. The latter is a natural extension to our previous work to the case of multiple calibrations and a birth-death process prior. However this extension turns out to be computationally expensive except for some special cases where a closed form formula exists. We therefore advocate the former approach (that always applies a uniform prior to ranked trees) as a practical alternative.

# 2 Methods

Consider the following notation:

$n$  Number of taxa.

$\Psi$  The set of all ranked binary topologies on  $n$  taxa. We keep  $n$  implicit to simplify the notation.

$\psi$  A ranked tree ( $\psi \in \Psi$ ).

$h = \{h_1, h_2, \dots, h_{n-1} : h_i \geq h_{i+1} \geq 0\}$ , an ordered set of divergence ages.

$g = \langle h, \psi \rangle$ , a time tree on  $n$  taxa.

$G$  the space of all time trees.

$\lambda$  the birth rate of the birth-death or Yule time tree prior.

$\mu$  the death rate of the birth-death time tree prior.

$\theta = \langle \Omega, r \rangle$ , a pair of parameter vectors, one for the substitution process  $\Omega$  and one for the rates of the molecular clock,  $r$ .

## 2.1 Posterior probability for Bayesian Inference

Without calibration, the posterior probability of  $(g, \Lambda, \theta)$  given a sequence alignment,  $D$  can be written:

$$f(g, \Lambda, \theta | D) = \frac{\Pr\{D|g, \theta\} f(\theta) f_G(g|\Lambda) f(\Lambda)}{\Pr\{D\}}. \quad (4)$$

The term  $\Pr\{D|g, \theta\}$  is the phylogenetic likelihood [Felsenstein, 1981]. The rates  $r$  and divergence times  $h$  combine to provide branch lengths in units of substitutions per site on the edges of  $\psi$ . The term  $f_G(g|\Lambda)$  is the uncalibrated tree prior and it can be readily factored in the following way:

$$f_G(g|\Lambda) = f(h|\Lambda) \Pr(\psi|\Lambda). \quad (5)$$

$f(h|\Lambda)$  is easy to compute for the pure birth (Yule) prior, birth-death prior or any prior whose equivalence classes are defined entirely by the divergence time order statistics. Under the Yule or birth-death prior *without calibrations*,  $\Pr(\psi|\Lambda) = |\Psi|^{-1}$ , is a uniform prior on all ranked topologies. However this factorisation is no longer simple when calibrations are introduced [Heled and Drummond, 2012], and so we must develop an alternative approach to describing the calibrated tree prior in the following sections, which we will call  $\rho_G(\cdot)$  to distinguish from the uncalibrated tree prior  $f_G(\cdot)$ . Note that throughout the remaining sections the tree priors are always conditional on  $\Lambda$ , but we suppress the conditioning in the notation for the sake of clarity.

## 2.2 Calibrated Birth-Death Density

We introduce some extra notation for calibrations:

$K$  Number of calibration points.

$\phi$  Set of conditions on  $\Psi$ , typically clade monophyly constraints.  $\phi$  plays a part in the terms defined below, but since it is fixed in each case we mostly keep it implicit to make the equations easier to read.

$\Psi_\phi$  The subset of all ranked topologies for which  $\phi$  holds.

$i(\psi) = (i_1, i_2, \dots, i_K)$ , mapping a ranked tree to the ranks of the calibrated nodes. Typically those are the ranks of the monophyletic clades in  $\phi$ , but  $i$  may, for example, pick the rank of a clade's parent instead.

We use two additional mappings which are a function of  $i$ .  $\bar{i}(\psi) = (\bar{i}_1, \bar{i}_2, \dots, \bar{i}_K)$  is the mapping of calibration ranks into their sort order. For example, if  $i = (3, 1, 4)$  then  $\bar{i} = (2, 1, 3)$  and if  $i = (7, 4, 2)$  then  $\bar{i} = (3, 2, 1)$ .

Also,  $\hat{i}(\psi) = (\hat{i}_1, \hat{i}_2, \dots, \hat{i}_K) = (i_{\bar{i}_1}, i_{\bar{i}_2}, \dots, i_{\bar{i}_K})$  are the ranks of the calibrated nodes sorted by age. For the two examples above we have respectively  $\hat{i} = (1, 3, 4)$  and  $(2, 4, 7)$ .

$h_\psi = (h_{i_1}, h_{i_1}, \dots, h_{i_K})$ , the heights of the calibration points on a given ranked tree  $\psi$ . For convenience  $g_\psi$  is the same as  $h_\psi$  when  $g = \langle h, \psi \rangle$ .

$\rho_h(h_\psi)$  A  $K$ -dimensional calibration density.

Figure 1 illustrates the main elements of our notation on an example tree with seven taxa and three calibrated sub-clades.

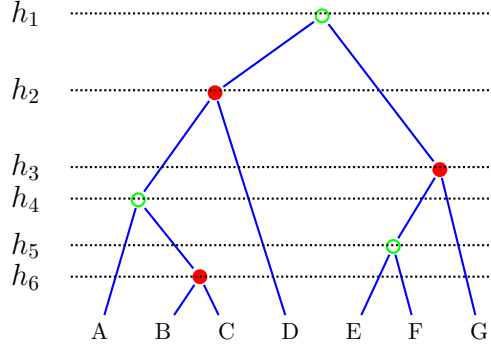


Figure 1: For the tree above we have:  $n = 7$  taxa, the ranked topology  $\psi = (((A,(B,C):1):3,D):5,((E,F):2,G):4)$  in NEWICK format, with internal nodes marked by rank,  $\phi = (\{E,F,G\}, \{B,C\}, \{A,B,C,D\})$ ,  $K = 3$  calibrated nodes marked in red, and  $i(\psi) = (3, 6, 2)$ ,  $\bar{i}(\psi) = (2, 3, 1)$ ,  $\hat{i}(\psi) = (2, 3, 6)$  and  $h_\psi = (h_3, h_6, h_2)$ .

In BEAST, the calibrated tree prior has been defined as,

$$\rho_G^{(M)}(g) \equiv f_G(g) \rho_h(h_\psi). \quad (6)$$

We shall call this the multiplicative prior, as designated by the superscript (M). While multiplying the two densities creates some valid (unnormalized) prior density, this tree prior fails to preserve the calibration density as the marginal prior distribution of the calibrated nodes. That is, the marginal calibration density – the density obtained by integrating out the non-calibrated heights over all time trees – is **not equal** to  $\rho_h$ .

In Heled and Drummond [2012] we showed that it is easy in principle to preserve the calibration marginal by scaling the prior with the conditional marginal value, that is, the total density of all trees whose calibration times are identical to the calibration times of  $g$ :

$$f_h(x) = \int_{\substack{g \in G \\ g_\psi = x}} f_G(g) dg. \quad (7)$$

The same general principle works for multiple calibrations:

$$\rho_G(g) \equiv f_G(g) \frac{\rho_h(h_\psi)}{f_h(h_\psi)}. \quad (8)$$

The notation for describing the calibrated prior is challenging because calibrated clade ages are not a simple subset of all ages. It may seem natural to define the joint density by defining the tree prior density as the product of conditional and calibration priors as done in Equation 3 of [Yang and Rannala, 2006] and mirrored in our own equation 3. But then Yang and Rannala deal only with trees whose ranked topology is known. For example, with this formulation one can easily forget that the space of possible values for the uncalibrated nodes depends on the tree topology and the calibrated nodes, and while this notational omission may be fine when the topology is fixed, it should be explicit when dealing with the whole of tree space. We think our notation is better suited for describing the properties of the prior in the context of the full tree space.

The conditional prior in equation (8) preserves the marginal by construction. This is easy to see by writing down the marginal density for  $x$ , a fixed vector of calibration values:

$$\int_{\substack{g \in G \\ h_\psi = x}} f_G(g) \frac{\rho_h(h_\psi)}{f_h(h_\psi)} dg = \int_{\substack{g \in G \\ h_\psi = x}} f_G(g) \frac{\rho_h(x)}{f_h(x)} dg = \rho_h(x) \frac{\int_{\substack{g \in G \\ h_\psi = x}} f_G(g) dg}{f_h(x)} = \rho_h(x). \quad (9)$$

However, the usefulness of this prior depends upon the computational cost of evaluating  $f_h(x)$  as part of the full posterior. In a few cases we can obtain a simple formula and the cost is negligible, and for the rest we offer either (a) a general algorithm for computing the marginal by iteration or (b) the *restricted conditional*, a fast alternate correction to be used when (a) is too slow. The iterative approach is based upon the *clade level partition*, which divides  $\Psi_\phi$  into disjoint subgroups whose marginal has a closed form, and we shall discuss the details later.

The restricted conditional prior is defined as follows

$$\rho_G^{(R)}(g = \langle \psi, h \rangle) \equiv f_G(g) \frac{\rho_h(h_\psi)}{f_h^{(R)}(h_\psi, \psi)}, \quad (10)$$

Where

$$f_h^{(R)}(x, \psi) = \int_{h_\psi = x} f_G(\langle \psi, h \rangle) dh. \quad (11)$$

Here the correction is defined as the marginal of the tree prior density when keeping **both** the topology and calibrated ages fixed. This is equivalent to extending the approach taken by Yang and Rannala [2006] to the case of an unknown tree topology. Again, the marginal over tree space is preserved by construction,

$$\begin{aligned} \int_{\substack{g = \langle \psi, h \rangle \in G \\ h_\psi = x}} f_G(g) \frac{\rho_h(h_\psi)}{f_h^{(R)}(h_\psi, \psi)} dg &= \sum_{\psi \in \Psi_\phi} \int_{\substack{g = \langle \psi, h \rangle \\ h_\psi = x}} f_G(g) \frac{\rho_h(x)}{f_h^{(R)}(x, \psi)} dh = \\ \rho_h(x) \sum_{\psi \in \Psi_\phi} \frac{1}{f_h^{(R)}(x, \psi)} \int_{\substack{g = \langle \psi, h \rangle \\ h_\psi = x}} f_G(g) dh &= \rho_h(x) \sum_{\psi \in \Psi_\phi} 1 \propto \rho_h(x). \end{aligned} \quad (12)$$

### 2.3 The Marginal Yule for Multiple Calibrations

We start by showing how to decompose the Yule density of genealogy  $g = \langle \psi, h \rangle$  conditional on  $\phi$ . The decomposition is based on separating the heights into  $r + 1$  *levels*, where each level spans the range between two consecutive calibration points.

The Yule density

$$f_G(h|\lambda) = \frac{1}{|\Psi_\phi|} n! e^{-\lambda h_1} \prod_{i=1}^{n-1} \lambda e^{-\lambda h_i} \quad (13)$$

is factored using the two propositions below.

**Proposition I:**

$$\begin{aligned} & \int_a^b dx_1 \int_a^{x_1} dx_2 \int_a^{x_2} dx_3 \cdots \int_a^{x_{k-1}} dx_k \lambda e^{-\lambda x_1} \lambda e^{-\lambda x_2} \cdots \lambda e^{-\lambda x_k} = \\ & \frac{1}{k!} \left[ \int_a^b \lambda e^{-\lambda x_1} dx_1 \right] \left[ \int_a^b \lambda e^{-\lambda x_2} dx_2 \right] \cdots \left[ \int_a^b \lambda e^{-\lambda x_k} dx_k \right] = \\ & \frac{1}{k!} (e^{-\lambda a} - e^{-\lambda b})^k \end{aligned} \quad (14)$$

**Proposition II:**

$$\begin{aligned} & \int_a^\infty dx_0 \int_a^{x_0} dx_1 \int_a^{x_1} dx_2 \cdots \int_a^{x_{k-1}} dx_k \lambda e^{-2\lambda x_0} \lambda e^{-\lambda x_1} \cdots \lambda e^{-\lambda x_k} \\ & \text{by proposition I} \\ & = \int_a^\infty \lambda e^{-2\lambda x_0} \frac{1}{k!} (e^{-\lambda a} - e^{-\lambda x_0})^k dx_0 \\ & \text{by equation (45)} \\ & = \frac{1}{(k+2)!} e^{-(k+2)\lambda a}. \end{aligned} \quad (15)$$

Proposition I gives the contribution of internal nodes located between two consecutive calibration points with ages  $a$  and  $b$ . Proposition II gives the contribution of nodes older than the last calibration point.

When the calibration values are fixed to  $x = (x_1, x_2, \dots, x_K)$ , the contribution of the ranked topology  $\psi$  is

$$\begin{aligned} f_h(x, \psi) = & \int_{\bar{x}_1}^\infty dh_1 \int_{\bar{x}_1}^{h_1} dh_2 \cdots \int_{\bar{x}_1}^{h_{\hat{i}_1-3}} dh_{\hat{i}_1-2} \int_{\bar{x}_1}^{h_{\hat{i}_1-2}} dh_{\hat{i}_1-1} \\ & \int_{\bar{x}_2}^{\bar{x}_1} dh_{\hat{i}_1+1} \int_{\bar{x}_2}^{h_{\hat{i}_1+1}} dh_{\hat{i}_1+2} \cdots \int_{\bar{x}_2}^{h_{\hat{i}_2-3}} dh_{\hat{i}_2-2} \int_{\bar{x}_2}^{h_{\hat{i}_2-2}} dh_{\hat{i}_2-1} \\ & \int_{\bar{x}_3}^{\bar{x}_2} dh_{\hat{i}_2+1} \int_{\bar{x}_3}^{h_{\hat{i}_2+1}} dh_{\hat{i}_2+2} \cdots \int_{\bar{x}_3}^{h_{\hat{i}_3-3}} dh_{\hat{i}_3-2} \int_{\bar{x}_3}^{h_{\hat{i}_3-2}} dh_{\hat{i}_3-1} \\ & \dots \\ & \int_0^{\bar{x}_K} dh_{\hat{i}_K+1} \int_0^{h_{\hat{i}_K+1}} dh_{\hat{i}_K+2} \cdots \int_0^{h_3} dh_2 \int_0^{h_2} dh_1 f_Y(\langle \psi, h \rangle). \end{aligned} \quad (16)$$

The above uses  $\bar{x} = (x_{\bar{i}_1}, x_{\bar{i}_2}, \dots, x_{\bar{i}_K})$ , the calibration height sorted by age. Now, let  $c_i$  be the number of internal nodes in each level,  $c_i = \hat{i}_{i+1} - \hat{i}_i - 1$  ( $0 \leq i \leq K$ ), and for convenience let  $\hat{i}_0 = 0$  and  $\hat{i}_K + 1 = n$ . Using propositions I and II we get

$$\begin{aligned} f_h(x, \psi) &= \frac{n!}{|\Psi_\phi|} \frac{e^{-(c_0+1)\lambda\bar{x}_1}}{(c_0+1)!} \\ &\quad \frac{\lambda e^{-\lambda\bar{x}_1}}{c_1!} \left(e^{-\lambda\bar{x}_2} - e^{-\lambda\bar{x}_1}\right)^{c_1} \frac{\lambda e^{-\lambda\bar{x}_2}}{c_2!} \left(e^{-\lambda\bar{x}_3} - e^{-\lambda\bar{x}_2}\right)^{c_2} \dots \frac{\lambda e^{-\lambda\bar{x}_K}}{c_K!} \left(e^{-0} - e^{-\lambda\bar{x}_K}\right)^{c_K} \\ &= \left[ \frac{n!}{|\Psi_\phi|} \prod_{k=1}^K \lambda e^{-\lambda\bar{x}_k} \right] \frac{e^{-(c_0+1)\lambda\bar{x}_1}}{(c_0+1)!} \prod_{k=1}^K \frac{\left(e^{-\lambda\bar{x}_{k+1}} - e^{-\lambda\bar{x}_k}\right)^{c_k}}{c_k!}. \end{aligned} \quad (17)$$

The marginal density is the sum over all **valid** topologies

$$f_h(x) = \sum_{\substack{\psi \in \Psi_\phi \\ \bar{i}(\psi) = \bar{i}(x)}} f_h(x, \psi). \quad (18)$$

To be valid, the order of calibration points by age has to be compatible with  $x$ .

While explicitly summing over all topologies is not feasible, evaluating the sum is possible by partitioning  $\Psi_\phi$  into  $\{\Psi_\phi^1, \Psi_\phi^2, \dots\}$ , where  $\psi_1, \psi_2 \in \Psi_\phi^k \implies i(\psi_1) = i(\psi_2)$ . That is, topologies in the same partition have the same number of internal nodes in each *level*. Since equation (17) depends only on those counts ( $c_i$ ) and not on the exact ranking, we have  $f_T(x, \psi_1) = f_T(x, \psi_2)$  for two topologies in the same partition. Finally,

$$f_h(x) = \sum_{\substack{\psi \in \Psi_\phi \\ \bar{i}(\psi) = \bar{i}(x)}} f_h(x, \psi) = \sum_{\substack{k \\ \bar{i}(\psi_k) = \bar{i}(x)}} |\Psi_\phi^k| f_h(x, \psi_k) \quad (19)$$

where  $\psi_k$  is any topology in  $\Psi_\phi^k$ .

## 2.4 The Marginal Birth-Death Prior for Multiple Calibrations

The birth-death process starts with a single species, and evolves over time through existing species giving birth (splitting) to new species at constant rate  $\lambda$  and dying (unobserved) at constant rate  $\mu$  [Kendall, 1948]. While this characterisation is unique, there are several versions of the prior which differ in their start and end conditions. BEAST uses the birth-death-sampling <sub>$\rho$</sub>  process, which assumes a uniform distribution  $[0, \infty]$  on the time of the tree origin, and that the leafs of the tree are sampled with probability  $\rho$  to obtain exactly  $n$  taxa. The density for this prior is given in equation (5) of [Stadler, 2009b]:

$$f_G(h|\lambda, \mu, \rho) = n!(\rho\lambda)^{n-1} \frac{(\lambda - \mu)e^{-(\lambda - \mu)h_1}}{\rho\lambda + (\lambda(1 - \rho) - \mu)e^{-(\lambda - \mu)h_1}} \prod_{i=1}^{n-1} \frac{(\lambda - \mu)^2 e^{-(\lambda - \mu)h_i}}{(\rho\lambda + (\lambda(1 - \rho) - \mu)e^{-(\lambda - \mu)h_i})^2}. \quad (20)$$

We obtain the marginal for the birth-death process using exactly the same procedure as described for the Yule, but using the birth-death analogous for propositions I and II. We use the following definitions for convenience:



$$\lambda' = \rho\lambda \quad (21)$$

$$\mu' = \mu - \lambda(1 - \rho) \quad (22)$$

$$q(t) = \frac{\lambda - \mu}{\lambda' - \mu' e^{-(\lambda - \mu)t}} \quad (23)$$

$$q_1(t) = e^{-(\lambda - \mu)t} q(t). \quad (24)$$

$$p_1(t) = q_1(t)q(t) \quad (25)$$

$p_1(t)$  is the probability that a lineage leaves one descendant after time  $t$ , which is easy to integrate

$$P_1(t) = \int p_1(t)dt = -\frac{q(t)}{\mu'}, \quad (26)$$

and gives us the birth-death equivalent of proposition I:

$$\int_a^b dx_1 \int_a^{x_1} dx_2 \dots \int_a^{x_{k-1}} dx_k \prod_{i=1}^k p_1(x_i) = \frac{1}{k!} (P_1(b) - P_1(a))^k. \quad (27)$$

For proposition II we have

$$\int_a^\infty dx_0 \int_a^{x_0} dx_1 \dots \int_a^{x_{k-1}} dx_k q_1(x_0) \prod_{i=0}^k p_1(x_i) = \frac{\lambda^{-(k+1)}}{(k+2)!} q_1(a)^{k+2} \quad (28)$$

Which is proved in the appendix. For the critical case  $\lambda = \mu$  we take the limit and use  $q_1(t) = \frac{1}{1+\lambda t}$  in the formulas above.

## 2.5 Partitioning and Counting

To evaluate the marginal (equation (19)) we need to establish a valid partitioning and count the number of ranked topologies in each partition. Ideally, the partition would be the smallest possible, that is  $\psi_1, \psi_2 \in \Psi_\phi^k \iff i(\psi_1) = i(\psi_2)$ . Unfortunately, we were unable to derive a counting formula under this constraint and instead use the clade level partition, a refinement based on the number of lineages per level inside each calibrated clade. Formally, let  $r(\psi) = \{r_1, r_2, \dots, r_K\}$  where  $r_j = (r_{j0}, r_{j1}, \dots, r_{jK})$  and  $r_{jk}$  is the number of sub-clades of the  $k^{th}$  calibration point whose rank is smaller than  $i_j$ . Since  $1 + \sum_k r_{jk} = i_j$ , the equivalence classes induced by  $r$  are a refinement of the ones induced by  $i(\cdot)$ . Furthermore, we can count the number of topologies in each class by using two generic combinatorial principles: first, the number of ways for lineages to coalesce in each level is independent of other levels, so the product of counts of all levels gives the total number of topologies. Second, when  $n = n_1 + n_2 + \dots + n_j$  lineages enter a level and are reduced to  $k = 1 + k_2 + \dots + k_j$ , where lineages can coalesce only within their group ( $n_i \rightarrow k_i$ ) and the root of the first group is calibrated ( $k_1 = 1$ ), the total number of ranked ways is  $\binom{n-k-1}{n_1-2, n_2-k_2, \dots, n_j-k_j} \prod_{i=1}^j R_{n_i}^{k_i}$ .

$R_n^k$  is the number of ranked ways  $n$  lineages can coalesce to  $k$  (equation (36)), and for convenience  $R_n = R_n^1$ .

Figure 2 illustrates the counting procedure on a small example tree.



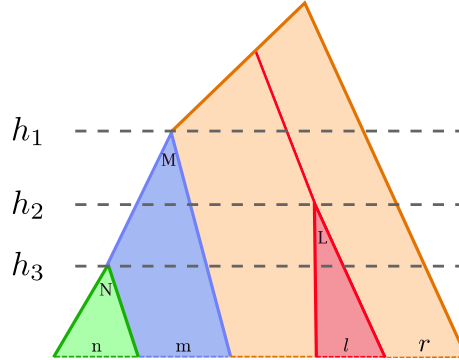


Figure 3: The calibrated clades are  $N$  (green),  $M$  (blue) and  $L$  (red), with respectively  $n + 2$ ,  $n + 2 + m + 1$  and  $l + 2$  taxa. In addition we have  $r$  “free” taxa in orange, which can coalesce between themselves and with the roots of  $M$  and  $L$ . There are 4 levels associated with the 3 calibration nodes, separated by the root ages of the calibrated clades.

The  $m + 1$  lineages of  $M$  not in  $N$  coalesce on the way to the clade root with each other and with the roots of the nested clades, in this case  $N$ . The  $r$  free lineages coalesce with the roots of  $L$  and  $M$  on the way up, and the internal nodes can be in any of the four levels.

Since there are 3 calibrations there are 4 levels, separated by the dashed lines, and each per-clade iterator returns 4 numbers. The iterator of  $N$  is trivial, always returning  $(n, 0, 0, 0)$ , since its root defines the first level. The iterator for  $L$  is simple too, since the lineages can coalesce only in the first two levels and there are no free lineages. The iterator returns  $(l, 0, 0, 0), (l - 1, 1, 0, 0), \dots, (0, l, 0, 0)$ .

The iterator for  $M$  takes care of  $m + 1$  free lineages which can coalesce in the first 3 levels. The iterator returns  $(m, 0, 0, 0), (m - 1, 1, 0, 0), (m - 1, 0, 1, 0), (m - 2, 2, 0, 0), (m - 2, 1, 1, 0), (m - 2, 0, 2, 0), \dots, (0, 0, m, 0)$ . Basically, the iterator first returns all the cases with  $m$  internal nodes in the first level, then all cases with  $m - 1$  internal nodes in the first level, and so on. The same pattern holds (recursively) for the rest of the levels.

The last iterator takes care of the  $r$  free lineages and the surviving lineages of any sub-clade, here the roots of  $M$  and  $L$ . In this example this iterator is only necessary if  $r > 0$ , as otherwise there are only two lineages left to deal with. While the internal nodes can be in any of the 4 levels, there are some restrictions. In general these restrictions can be quite involved. In this example, the restrictions arise because the enclosing clade (here the root of the tree) has more than one monophyletic sub-clade. As a result we always have at least three lineages above  $h_2$ , and since only 2 lineages coalesce at the root, the excess has to coalesce in the top 2 levels. So, the iterator returns  $(r - 1, 0, 1, 0), (r - 1, 0, 0, 1), (r - 2, 1, 1, 0), \dots, (0, 0, 0, r)$ , filling up lower levels first as before, while keeping at least one event in the top two.

### 3 Results

#### 3.1 Calibrating the Parent of One Monophyletic Clade

Sometimes the calibration information is about the time a particular clade (say a genera, or a species which is divided into sub-species) separated from other lineages in the tree. For a single lineage, the density is given in Heled and Drummond [2012]

$$f_h(x) = 2\lambda e^{-2\lambda x}. \quad (29)$$

Note that the parent age is equal to the (pendant) branch length, and in fact  $f_h(x)$  is the distribution of the branch length when conditioning on the number of leaves. Furthermore, since this holds for any branch, we can derive a mean of  $1/2\lambda$ , which reproduces a result discussed by Steel and Mooers [2010].

The result can be generalized to any clade  $C$  of size  $n$ . In that case  $\Psi_\phi$  to be the set of all genealogies of  $n + l$  taxa with a monophyletic clade on  $n$  taxa ( $n > 1$  and  $l > 0$ ) (Figure 4).

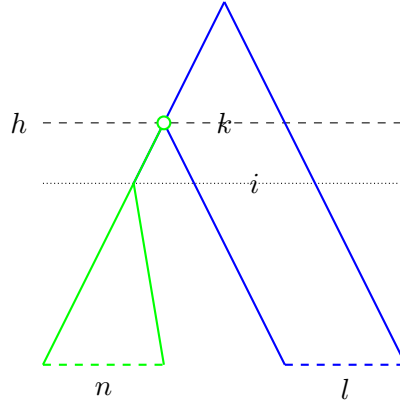


Figure 4: Parent of monophyletic clade of size  $n$ .

We partition  $\Psi_\phi$  so that  $\Psi_\phi^k$  contains all genealogies containing  $k + 1$  surviving lineages at  $h$ , the age of the calibrated parent. By the second counting principle, there are  $R_n R_l^i \binom{n-2+l-i}{n-2}$  ranked ways for lineages to coalesce in the first level,  $R_i^{k+1}$  ways for  $i$  lineages to reduce to  $k + 1$  in the second level, and then one of the  $k + 1$  coalesce with the parent of  $C$ . Then  $k + 1$  lineages coalesce to the root, giving

$$\begin{aligned} |\Psi_\phi^k| &= \sum_{i=k+1}^l R_n R_l^i \binom{n-2+l-i}{n-2} (k+1) R_i^{k+1} R_{k+1} \\ &= (k+1) \binom{n-2+l-k}{n-1} R_n R_l. \end{aligned} \quad (30)$$

The total number of ranked trees in  $\Psi_\phi$  is

$$|\Psi_\phi| = \sum_{k=0}^{l-1} |\Psi_\phi^k| = \binom{l+n}{l-1} R_l R_n. \quad (31)$$

Putting it all together,

$$\begin{aligned}
f_h(x) &= \frac{1}{|\Psi_\phi|} \sum_{k=0}^{l-1} |\Psi_\phi^k| (n+l)! \\
&\quad e^{-\lambda x} \frac{e^{-(k+1)\lambda x}}{(k+1)!} \frac{(1 - e^{-\lambda x})^{n+l-k-2}}{(n+l-k-2)!} \\
&= n(n+1) \sum_{k=0}^{l-1} \binom{l-1}{k} e^{-(k+2)\lambda x} (1 - e^{-\lambda x})^{n+l-(k+2)} \\
&= n(n+1) \lambda e^{-2\lambda x} (1 - e^{-\lambda x})^{n-1}.
\end{aligned} \tag{32}$$

Note that the marginal does not depend the size of the tree, just on the size of the calibrated clade.

### 3.2 Calibrating Two Nested Clades

Here we give the marginal density for two nested clades. When the enclosing clade is the root (Figure 5), the marginal is

$$\begin{aligned}
f_h(h_0, h|n, m) &= (n-1)n(n+1)\lambda^2 e^{-\lambda(h+2h_0)} (1 - e^{-\lambda h})^{n-2} (1 - e^{-\lambda h_0})^{m-3} \\
&\quad \left[ 1 + 2(m-1)e^{-\lambda h} - 2me^{-\lambda h_0} - m(m-1)e^{-\lambda(h_0+h)} + \binom{m-2}{2} e^{-2\lambda h} + \binom{m}{2} e^{-2\lambda h_0} \right],
\end{aligned} \tag{33}$$

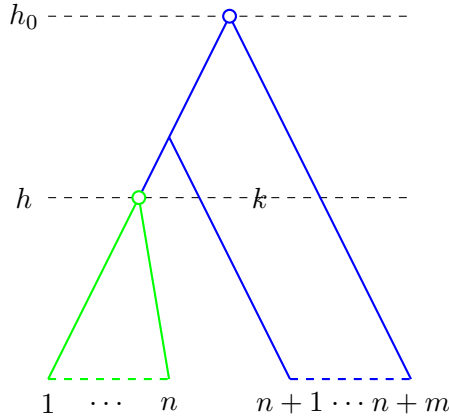


Figure 5: Monophyletic clade of size  $n$  and root with  $n+m$  taxa.

And when the enclosing clade is proper (Figure 6), it is

$$\begin{aligned}
f_h(h_1, h_2|n, m) &= \frac{1}{2}(n-1)n(n+1)(n+1+m)\lambda^2 e^{-\lambda(h_2+3h_1)} (1 - e^{-\lambda h_2})^{n-2} (1 - e^{-\lambda h_1})^{m-3} \\
&\quad \left[ 1 - 2me^{-\lambda h_1} + 2(m-1)e^{-\lambda h_2} - m(m-1)e^{-\lambda(h_2+h_1)} + \binom{m+1}{2} e^{-2\lambda h_1} + \binom{m-1}{2} e^{-2\lambda h_2} \right].
\end{aligned} \tag{34}$$

See the appendix for additional details on the derivation of those formulas.

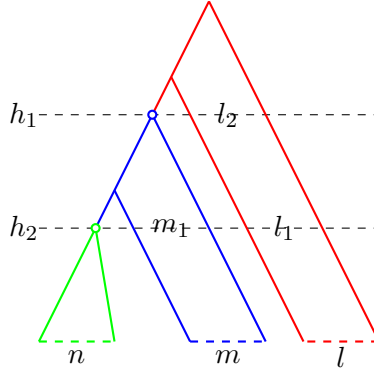


Figure 6: Two nested monophyletic clades of size  $n$  and  $n + m$  taxa in a  $n + m + l$  taxa tree ( $l > 0$ ).

### 3.3 Placing Additional Monophyly Constraints

It is important to keep in mind that placing additional constraints can invalidate the closed form equations for the marginal. However, it still may be possible to obtain formula for the full set of constraints. For example, the marginal density for a monophyletic clade of size  $n$  in a  $n + m + 1$  taxa tree with an outgroup can be obtained by integrating out  $h_2$  in equation (34) and is equal to

$$f_h(x) = \frac{(n-1)n(n+1)(n+m+1)}{m(m+1)(m+2)} \lambda e^{-\lambda x} (1 - e^{-\lambda x})^{n-2} \left( 1 - (1 - e^{-\lambda x})^{m+2} - (m+2)e^{-\lambda x} + \binom{m+2}{2} e^{-2\lambda x} \right), \quad (35)$$

which is not equal to the marginal for the same sized tree where the monophyly on the  $n + m$  clade is not enforced.

We can also derive the marginal in some cases which are not covered by the standard construction (root ages of monophyletic clades and no extra constraints). For example, take the \*BEAST analysis performed as part of the investigation of determining the Pipid root [Bewick et al., 2012]. This analysis involves the species *Xenopus*, *Silurana*, *Hymenochirus*, *Pipa* and an outgroup. Five species in total with a 4 taxa monophyly and a calibration on the age of the parent of *Pipa*. There are  $6 \times 3$  valid ranked topologies: 9 of those have 3 internal nodes above the calibrated parent, 6 has 2 above and 1 below, and the remaining 3 has 2 below and one (the root) above.

The total density for  $a$  internal nodes above and  $b$  below by equation (17) is

$$f_{a,b}(h) = \lambda e^{-\lambda h} \frac{e^{-\lambda(a+1)h} (1 - e^{-\lambda h})^b}{(a+1)! b!},$$

and so the marginal is:

$$\begin{aligned} f_h(h) &= \frac{5!}{18} (9f_{3,0}(h) + 6f_{2,1}(h) + 3f_{1,2}(h)) \\ &= \frac{5\lambda e^{-3\lambda h}}{6} (e^{-2\lambda h} - 4e^{-\lambda h} + 6). \end{aligned}$$

### 3.4 A four taxon tree with one calibration

Following Heled and Drummond (2012) we consider the following four taxa tree in which taxa A,B are constrained to be monophyletic and their most recent common ancestor is calibrated with density  $f_{AB}$ .

There are 4 ranked topologies in this case, and the 2012 article gives the marginal density for each. Here we wish to contrast the three priors using concrete values: a birth rate of  $\lambda = 1/2$  and a uniform calibration prior ( $f_{AB} = U[4, 6]$ ). Table 1 summarises the results.

		Multiplicative	Conditional	Restricted conditional
Prior “correction term”	$((A,B),(C,D)) \ T_{CD} < T_{AB}$	–	$3\lambda e^{-3\lambda h_2}$	$12e^{-3\lambda h_2}(1 - e^{-\lambda h_2})$
	$((A,B),(C,D)) \ T_{CD} \geq T_{AB}$			
	$((A,B),C),D)$	–	$3\lambda e^{-3\lambda h_3}$	$4\lambda e^{-4\lambda h_3}$
	$((A,B),D),C)$			
Marginal Topology probability	$((A,B),(C,D))$	93%	94.2%	50%
	$((A,B),C),D)$	3.5%	2.9%	25%
	$((A,B),D),C)$	3.5%	2.9%	25%
Marginal calibration prior		$\frac{3\lambda e^{-3\lambda x}}{e^{-12\lambda} - e^{-18\lambda}}$	$\frac{1}{6-4}$	$\frac{1}{6-4}$

Table 1: An illustration of the difference between the restricted and full conditional prior using a 4 taxa example. The prior is a pure birth process with a birth rate of  $\lambda = 1/2$  and a uniform calibration density between 4 and 6 is applied to the monophyletic clade (A,B). The uncorrected (multiplicative) prior is  $\frac{1}{6-4}4!\lambda^3 e^{-\lambda(2h_1+h_2+h_3)}$ , and the table gives the conditional prior “correction terms” for each ranked topology, together with the induced prior probability of each unranked topology and the marginal density for the calibrated clade.

The table lists the “correction term” for each ranked topology, the marginal probability for each unranked topology and the calibration marginal. As expected, the full and restricted conditional preserve the calibration density, while the marginal for the multiplicative prior is equal to the conditional marginal ( $3\lambda e^{-3\lambda x}$ ), bounded between 4 and 6. The marginal topology probability illustrates the difference between the full and restricted priors. The former is similar to the multiplicative prior, with a high probability on the balanced tree. In the space of Yule trees with birth rate  $1/2$  and one internal node age between 4 and 6, the other age is far more likely to be smaller than the first. The latter, with equal weight for the two classes, matches the probabilities of the Yule prior without calibration.

### 3.5 Three Calibrations for Bombina

A recent study using 13 complete genomes investigated the phylogenetic relationships of the firebellied toads of the genus *Bombina* [Pabijan et al., 2013]. The study contains many kinds of analysis, using different calibration schemes. One BEAST analysis used three nested calibration points, on 5 taxa, 7 taxa and the root. The results of running only the multiplicative prior are shown in figure 7 (a).

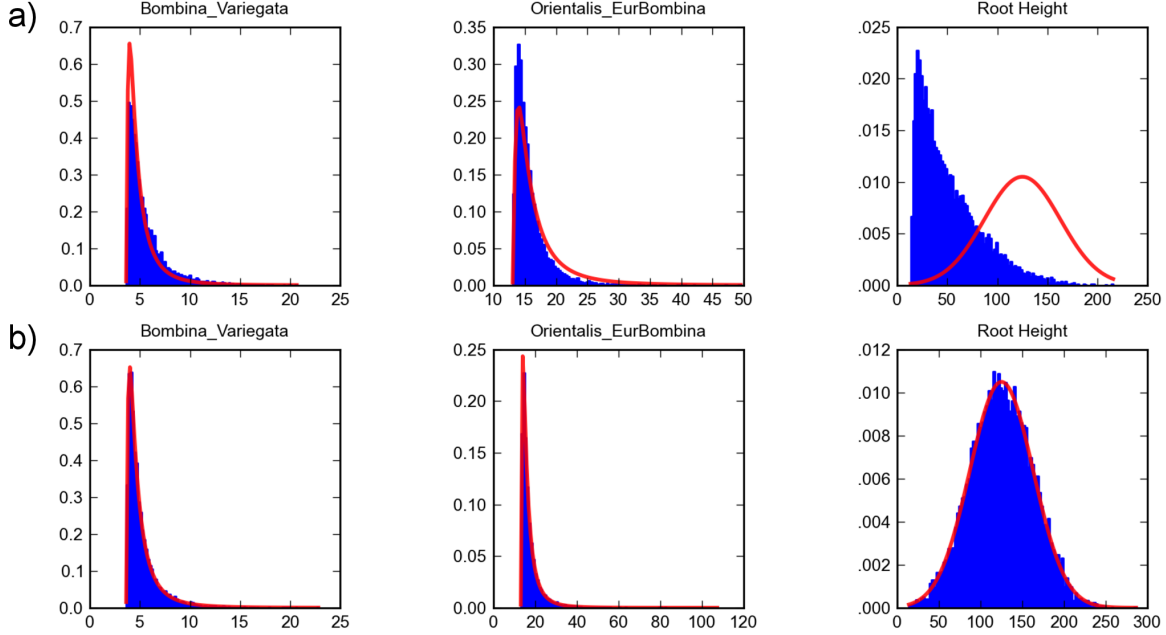


Figure 7: Three calibration densities for the Bombina analysis, (a) under BEAST multiplicative calibration prior and (b) under the conditional prior. The specified densities are in red, and the blue show the density from a BEAST run.

While the marginal for the two clades deviate only slightly from the calibration, the marginal for the root, with mean around 50, is way off from the normal density calibration ( $N(125,36)$ ). The marginals for the analysis using the conditional prior described here match the calibration densities as expected (Figure 7 (b)).

## 4 Conclusions

We have presented a general approach to specifying a birth-death process tree prior conditional on the heights of a set of calibrated nodes, in the context of the joint inference of topology and divergence times. We have described a few special cases where this prior density has a closed form solution and we have described a general, though computationally intensive, approach to numerical calculation of this conditional density for any number of calibrated nodes. As a result, an arbitrary marginal prior distribution can be precisely specified on the calibrated nodes.

We have also described how the conditional birth-death tree prior naturally induces a non-uniform distribution over ranked topologies. If this effect is unwanted, our approach can be modified to produce a uniform prior on ranked topologies (therefore permitting any arbitrary distribution on ranked tree topologies to be composed with the conditional birth-death prior on divergence times). This modification also renders a computationally efficient algorithm for calculation of the prior density.

In order to compute the conditional birth-death prior, it is necessary to compute the marginal density of the calibrated node heights averaged over all consistent time-trees. Although we have



described some special cases where this marginal prior density of the calibrated nodes can be efficiently computed, it remains to be determined whether other cases have analytical closed-form solutions.

Our implementation is available in BEAST2 (<http://code.google.com/p/beast2/>). We regard the full conditional formulation as the correct approach, if one assumes that the birth-death process prior is the appropriate prior for the phylogenetic time-tree under estimation. We therefore recommend the full conditional formulation when computationally feasible (e.g. 2-3 calibrations and/or small numbers of taxa). The restricted formulation effectively removes influence of the birth-death prior on the estimation of the ranked topology and is a good alternative for analyses with large numbers of calibrations or taxa for which computational considerations will preclude application of the full conditional. Both of these approaches relieve the practitioner from running their calibrated analysis in the absence of data in order to determine the resulting marginal distributions (e.g. compare Fig 7a and Fig 7b).

It is clear that development of calibrated tree priors for Bayesian phylogenetic inference remains an area ripe for future development. Obvious next steps would include taking explicitly account of the different sources of uncertainty in fossil ages and collection (uncertainty in geological dates, variation in fossil preservation rates and paleontological discovery effort) and more sophisticated means of dealing with the phylogenetic placement of fossil information (uncertain placement of fossils based on morphological characters of fossils and/or tree process prior assumptions). All of these factors are currently subsumed into whatever marginal distribution is specified on the set of calibrated nodes. In the mean time the work presented here derives new results for multiple-calibration tree priors and in doing so illustrates some of the subtle choices open to the practitioner when calibrating birth-death tree priors.

## 5 Authors contributions

AJD and JH designed the study. JH designed the algorithm for computation of full conditional formulation. AJD proposed the solution for the restricted conditional formulation. JH produced all derivations and performed all data analyses. AJD and JH produced the figures and wrote the manuscript.

## 6 Acknowledgements

The authors wish to thank Mike Steel for helpful discussion and comments. JH and AJD were supported by a Rutherford Discovery Fellowship from the Royal Society of New Zealand awarded to AJD.

## References

- Adam J Bewick, Frédéric JJ Chain, Joseph Heled, and Ben J Evans. The pipid root. *Systematic Biology*, 61(6):913–926, 2012.
- A.J Drummond and A Rambaut. Beast: Bayesian evolutionary analysis by sampling trees. *BMC Evol Biol*, 7:214, 2007. ISSN 1471-2148 (Electronic). doi: 10.1186/1471-2148-7-214.

- AJ Drummond, SYW Ho, MJ Phillips, and A. Rambaut. Relaxed phylogenetics and dating with confidence. *PLoS Biol*, 4(5):e88, 2006.
- J. Felsenstein. Evolutionary trees from DNA sequences: a maximum likelihood approach. *Journal of molecular evolution*, 17(6):368–376, 1981.
- T. Gernhard. The conditioned reconstructed process. *Journal of Theoretical Biology*, 253(4):769–778, 2008.
- Joseph Heled and Alexei J. Drummond. Calibrated tree priors for relaxed phylogenetics and divergence time estimation. *Systematic Biology*, 61(1):138–149, 2012.
- Sebastian Höhna, Tanja Stadler, Fredrik Ronquist, and Tom Britton. Inferring speciation and extinction rates under different sampling schemes. *Mol Biol Evol*, 28(9):2577–89, Sep 2011. doi: 10.1093/molbev/msr095.
- J.P. Huelsenbeck and F. Ronquist. MRBAYES: Bayesian inference of phylogenetic trees, 2001.
- David G Kendall. On the generalized” birth-and-death” process. *The annals of mathematical statistics*, pages 1–15, 1948.
- Hirohisa Kishino, Jeffrey L. Thorne, and William J. Bruno. Performance of a divergence time estimation method under a probabilistic model of rate evolution. *Molecular Biology and Evolution*, 18(3):352–361, 2001. URL <http://mbe.oxfordjournals.org/cgi/content/abstract/18/3/352>.
- S Nee, E C Holmes, R M May, and P H Harvey. Extinction rates can be estimated from molecular phylogenies. *Philos Trans R Soc Lond B Biol Sci*, 344(1307):77–82, Apr 1994a. doi: 10.1098/rstb.1994.0054.
- S Nee, R M May, and P H Harvey. The reconstructed evolutionary process. *Philos Trans R Soc Lond B Biol Sci*, 344(1309):305–11, May 1994b. doi: 10.1098/rstb.1994.0068.
- Maciej Pabijan, Anna Wandycz, Sebastian Hofman, Karolina Wecek, Marcin Piwczyński, and Jacek M Szymura. Complete mitochondrial genomes resolve phylogenetic relationships within *i*<sub>l</sub> bombina*i*/*i*<sub>l</sub>(anura: Bombinatoridae). *Molecular phylogenetics and evolution*, 2013.
- B Rannala and Z Yang. Probability distribution of molecular evolutionary trees: a new method of phylogenetic inference. *J Mol Evol*, 43(3):304–11, Sep 1996.
- Bruce Rannala and Ziheng Yang. Inferring speciation times under an episodic molecular clock. *Systematic Biology*, 56(3):453–466, 2007.
- Renzo Sprugnoli. An introduction to mathematical methods in combinatorics. *Dipartimento di Sistemi e Informatica Viale Morgagni*, 2006.
- Tanja Stadler. On incomplete sampling under birth-death models and connections to the sampling-based coalescent. *J Theor Biol*, 261(1):58–66, Nov 2009a. doi: 10.1016/j.jtbi.2009.07.018.
- Tanja Stadler. On incomplete sampling under birth–death models and connections to the sampling-based coalescent. *Journal of Theoretical Biology*, 261(1):58–66, 2009b.

- Mike Steel and Arne Mooers. The expected length of pendant and interior edges of a yule tree. *Applied Mathematics Letters*, 23:1315–1319, 2010. doi: DOI10.1016/j.aml.2010.06.021.
- Jeffrey L Thorne and Hirohisa Kishino. Divergence time and evolutionary rate estimation with multilocus data. *Syst Biol*, 51(5):689–702, 2002. ISSN 1063-5157 (Print). doi: 10.1080/10635150290102456.
- J.L. Thorne, H. Kishino, and I.S. Painter. Estimating the rate of evolution of the rate of molecular evolution. *Molecular Biology and Evolution*, 15:1647–1657, 1998.
- Z Yang and B Rannala. Bayesian phylogenetic inference using dna sequences: a markov chain monte carlo method. *Mol Biol Evol*, 14(7):717–24, Jul 1997.
- Ziheng Yang and Bruce Rannala. Bayesian estimation of species divergence times under a molecular clock using multiple fossil calibrations with soft bounds. *Molecular Biology and Evolution*, 23(1): 212–226, 2006.
- G.U. Yule. A mathematical theory of evolution based on the conclusions of dr. j.c. willis. *Philosophical Transactions of the Royal Society of London, Series B*, 213:21–87, 1924.

## A Two Monophyletic Nested Clades for the Yule Prior

$R_n^k$  is the number of ranked ways  $n$  lineages can coalesce to  $k$

$$\begin{aligned} R_n &= \prod_{i=2}^n \binom{i}{2} = \frac{n!(n-1)!}{2^{n-1}} \\ R_n^k &= \prod_{i=k+1}^n \binom{i}{2} = \frac{R_n}{R_k} = 2^{-(n-k)} \frac{n(n-1)!^2}{k(k-1)!^2} \end{aligned} \tag{36}$$

### A.1 Root and Clade

For the marginal of a monophyletic clade of  $n$  taxa and the root in a  $n + m$  taxa tree we partition  $\Psi_\phi$  so that  $\Psi_\phi^k$  contain all topologies with  $k + 1$  surviving lineages at time  $h$  (Figure 5).

The size of each subset is

$$|\Psi_\phi^k| = \binom{n-2+l-k}{n-2} R_n R_l^k R_{k+1} \tag{37}$$

and from (Heled and Drummond [2012] appendix C, equation (12)) we have

$$|\Psi_\phi| = \binom{n+l}{l-1} R_l R_n. \tag{38}$$

Plugging those counts into equation (19) we get

$$\begin{aligned}
& \frac{1}{|\Psi_\phi|} \sum_{k=1}^l \left[ |\Psi_\phi^k| (n+l)! \lambda e^{-\lambda h} \lambda e^{-2\lambda h_0} \right. \\
& \quad \left. \frac{(1 - e^{-\lambda h})^{n-2+l-k}}{(n-2+l-k)!} \frac{(e^{\lambda h} - e^{\lambda h_0})^{k-1}}{(k-1)!} \right] = \\
& (n-1)n(n+1) \sum_{k=1}^l \left[ \binom{k+1}{2} \binom{l-1}{k-1} \lambda e^{-\lambda h} \lambda e^{-2\lambda h_0} \right. \\
& \quad \left. (1 - e^{-\lambda h})^{n-2+l-k} (e^{\lambda h} - e^{\lambda h_0})^{k-1} \right] = \\
& (n-1)n(n+1) \lambda^2 e^{-\lambda(h+2h_0)} (1 - e^{-\lambda h})^{n-2} \\
& \quad \sum_{k=1}^l \binom{k+1}{2} \binom{l-1}{k-1} (1 - e^{-\lambda h})^{l-k} (e^{\lambda h} - e^{\lambda h_0})^{k-1},
\end{aligned} \tag{39}$$

which simplifies to equation (33), because without the  $\binom{k+1}{2}$ , the sum is the binomial expansion of  $(u+v)^{l-1}$ , and with the combinatorial identity

$$\sum_{k=0}^n \binom{k}{m} \binom{n}{k} u^k v^{n-k} = \binom{n}{m} u^m (u+v)^{n-m}, \tag{40}$$

we can simplify such sums where the terms are multiplied by any simple polynomial in  $k$ .

$(x)_n$  is the Pochhammer symbol, the falling factorial. Here  $\binom{k+1}{2} = \frac{1}{2}(k)_2 + (k)_1$ .

## A.2 Two Nested Clades

When the top clade is not the root we need to handle 3 levels. Let the number of surviving lineages at  $h_2$  be  $m_1$  and  $l_1$ , and  $l_2$  at  $h_1$  (Figure 6). We partition  $\Psi_\phi$  according to  $m_1$ ,  $l_1$  and  $l_2$ . that is topologies with the equal values are in the same class.

The number of internal nodes at the three levels is

$$\begin{aligned}
k_0 &= n + m + l - (m_1 + l_1 + 2) \\
k_1 &= m_1 + l_1 - (1 + l_2) \\
k_2 &= l_2 + 1 - 1.
\end{aligned}$$

The size of each subset is

$$\begin{aligned}
|\Psi_\phi^{m_1, l_1, l_2}| &= R_n R_m^{m_1} R_l^{l_1} \frac{k_0!}{(n-2)!(m-m_1)!(l-l_1)!} \\
& R_{m_1+1} R_{l_1}^{l_2} \binom{k_1}{m_1-1} \\
& R_{l_2+1}.
\end{aligned} \tag{41}$$

Each of the 3 lines above gives the contribution of one level. The total number of topologies is

$$|\Psi_\phi| = \binom{n+m}{m-1} R_m R_n \binom{n+m+l}{l-1} R_l. \tag{42}$$

This can be obtained either from summing over all  $\Psi_\phi^{m_1, l_1, l_2}$  terms or more simply by applying equation (38) twice, since the internal clade  $N$  does not interact with the free global lineages. Again pluggin those counts into equation (17) we get

$$f_{m_1, l_1, l_2}(h_1, h_2) = (n + m + l)! \lambda^2 e^{-\lambda(h_2 + h_1)} \frac{e^{-(k_2 + 1)\lambda h_1}}{(k_2 + 1)!} \frac{(1 - e^{-\lambda h_2})^{k_0}}{k_0!} \frac{(e^{-\lambda h_2} - e^{-\lambda h_1})^{k_1}}{k_1!}. \quad (43)$$

And finally

$$f(h_1, h_2) = |\Psi_\phi|^{-1} \sum_{m_1=1}^m \sum_{l_1=1}^l \sum_{l_2=1}^{l_1} |\Psi_\phi^{m_1, l_1, l_2}| f_{m_1, l_1, l_2}. \quad (44)$$

The rest is tedious manipulations similar to those in the root and clade case above.

## B Integral Identity used in Obtaining the Yule Marginal

$$\int_h^\infty n \lambda e^{-n \lambda x} (e^{-\lambda h} - e^{-\lambda x})^m dx = \binom{m+n}{n}^{-1} e^{-(m+n)\lambda h} \quad (45)$$

Proof:

$$\begin{aligned} \int_h^\infty n \lambda e^{-n \lambda x} (e^{-\lambda h} - e^{-\lambda x})^m dx &= \int_h^\infty n \lambda e^{-n \lambda x} e^{-m \lambda h} (1 - e^{-\lambda(x-h)})^m dx \\ &= \int_h^\infty n \lambda e^{-n \lambda x} e^{-m \lambda h} \sum_{k=0}^m (-1)^k \binom{m}{k} e^{-k \lambda(x-h)} dx \\ &= n \lambda e^{-m \lambda h} \sum_{k=0}^m (-1)^k \binom{m}{k} e^{\lambda k h} \int_h^\infty e^{-(k+n)\lambda x} dx \\ &= n \lambda e^{-m \lambda h} \sum_{k=0}^m (-1)^k \binom{m}{k} e^{\lambda k h} \frac{e^{-(k+n)\lambda h}}{(k+n)\lambda} \\ &= e^{-(m+n)\lambda h} \sum_{k=0}^m (-1)^k \binom{m}{k} \frac{n}{(k+n)} \quad \text{Using (46)} \\ &= e^{-(m+n)\lambda h} \binom{m+n}{n}^{-1} \end{aligned}$$

The last step used the well known combinatorial identity (for example, Sprugnoli [2006], page 74)

$$\sum_{k=0}^m (-1)^k \binom{m}{k} \frac{n}{n+k} = \binom{m+n}{n}^{-1}. \quad (46)$$

## C The Birth-Death Prior Marginal

For convenience, let  $z = x_{i_1}$  be the age of the last calibration point, and  $\hat{c} = c_1 - 1$ , the number of lineages between the root and the last calibration point (excluding the root).

$$\begin{aligned}
P_0(z) &= \int_z^\infty \int_z^{x_1} \cdots \int_z^{x_{\hat{c}}} \left[ q_1(x_1) \prod_{k=1}^{\hat{c}+1} p_1(x_k) \right] dx = \\
&= \int_z^\infty \left[ q_1(x_1) p_1(x_1) \frac{(P_1(x_1) - P_1(z))^{\hat{c}}}{\hat{c}!} \right] dx_1 = \\
&= \frac{1}{\hat{c}!} \int_z^\infty q_1(x_1) p_1(x_1) \sum_{j=0}^{\hat{c}} \binom{\hat{c}}{j} P_1(x_1)^j (-P_1(z))^{\hat{c}-j} dx_1 = \\
&= \frac{1}{\hat{c}!} \sum_{j=0}^{\hat{c}} (-P_1(z))^{\hat{c}-j} \binom{\hat{c}}{j} \int_z^\infty q_1(x_1) p_1(x_1) P_1(x_1)^j dx_1.
\end{aligned} \tag{47}$$

The following solution for the integral can be verified by taking the derivative of the right hand side

$$\begin{aligned}
\int q_1(x_1) p_1(x_1) P_1(x_1)^j dx_1 &= \frac{1}{(j+1)(j+2)} \left( \frac{\mu - \lambda}{\mu'} \right)^{j+2} \frac{\lambda' - (j+2)\mu' e^{-(\lambda-\mu)x_1}}{(\lambda' - \mu' e^{-(\lambda-\mu)x_1})^{j+2}} \\
&= \frac{\mu'^{-(j+2)}}{(j+1)(j+2)} (\lambda' - (j+2)\mu' e^{-(\lambda-\mu)x_1}) q(x_1)^{j+2}.
\end{aligned}$$

Substituting in Eq. (47) and simplifying gives

$$\begin{aligned}
P_0(z, x_1) &= \frac{1}{\hat{c}!} \sum_{j=0}^{\hat{c}} (-P_1(z))^{\hat{c}-j} \binom{\hat{c}}{j} \frac{\mu'^{-(j+2)}}{(j+1)(j+2)} (\lambda' - (j+2)\mu' e^{-(\lambda-\mu)x_1}) q(x_1)^{j+2} = \\
&= \frac{1}{\hat{c}!} \sum_{j=0}^{\hat{c}} \left( \frac{-q(z)}{\mu'} \right)^{\hat{c}-j} \binom{\hat{c}}{j} \frac{\mu'^{-(j+2)}}{(j+1)(j+2)} (\lambda' - (j+2)\mu' e^{(\lambda-\mu)x_1}) q(x_1)^{j+2} = \\
&= \frac{\mu'^{-(\hat{c}+2)}}{(\hat{c}+2)!} \sum_{j=0}^{\hat{c}} \binom{\hat{c}+2}{j+2} (-q(z))^{\hat{c}-j} (\lambda' - (j+2)\mu' e^{(\lambda-\mu)x_1}) q(x_1)^{j+2} = \\
&= \frac{\mu'^{-(\hat{c}+2)}}{(\hat{c}+2)!} \left[ \sum_{j=0}^{\hat{c}} \lambda' \binom{\hat{c}+2}{j+2} (-q(z))^{\hat{c}-j} q(x_1)^{j+2} - \sum_{j=0}^{\hat{c}} -(j+2) \binom{\hat{c}+2}{j+2} \mu' e^{(\lambda-\mu)x_1} (-q(z))^{\hat{c}-j} q(x_1)^{j+2} \right] = \\
&= \frac{\mu'^{-(\hat{c}+2)}}{(\hat{c}+2)!} \lambda' \left( (q(x_1) + q(z))^{\hat{c}+2} - (-q(z))^{\hat{c}+2} - (\hat{c}+2) q(x_1) (-q(z))^{\hat{c}+1} \right) \\
&\quad + \left( (\hat{c}+2) q(x_1) ((-q(z))^{\hat{c}+1} - (q(x_1) + q(z))^{\hat{c}+1}) \right).
\end{aligned} \tag{48}$$

The last step uses Equation (40) for the second sum. Now, after canceling terms and simplifying we are left with

$$P_0(z) = P_0(z, x_1) \Big|_{x_1=z}^{\infty} = \frac{\lambda' - (k+1)}{(k+2)!} q_1(z)^{k+2}. \quad (49)$$